Check for updates

Interdimensional radial discrete diffraction in Mathieu photonic lattices

JADRANKA M. VASILJEVIĆ,[1,*] (iD) VLADIMIR P. JOVANOVIĆ,[2]
ALEKSANDAR Ž. TOMOVIĆ,[2] DEJAN V. TIMOTIJEVIĆ,[2] RADOMIR
ŽIKIC,[2] MILIVOJ R. BELIĆ,[3] AND DRAGANA M. JOVIĆ SAVIĆ[1]

[1] *Institute of Physics, University of Belgrade, P.O. Box 68, 11001 Belgrade, Serbia*
[2] *Institute for Multidisciplinary Research, University of Belgrade, Kneza Višeslava 1, 11030, Belgrade, Serbia*
[3] *Division of Arts and Sciences, Texas A & M University at Qatar, 23874, Doha, Qatar*
[*] jadranka@ipb.ac.rs

Abstract: We demonstrate transitional dimensionality of discrete diffraction in radial-elliptical photonic lattices. Varying the order, characteristic structure size, and ellipticity of the Mathieu beams used for the photonic lattices generation, we control the shape of discrete diffraction distribution over the combination of the radial direction with the circular, elliptic, or hyperbolic. We also investigate the transition from one-dimensional to two-dimensional discrete diffraction by varying the input probe beam position. The most pronounced discrete diffraction is observed along the crystal anisotropy direction.

1. Introduction

The ability to tailor and manipulate light in photonic lattices is an important topic of scientific investigations and practical applications in optics [1]. Photonic lattices or arrays of evanescently coupled waveguides are typical examples of structures where discrete effects and dynamics can be investigated. Light focused into one waveguide that linearly propagates along the waveguide array will tunnel to neighboring sites, exhibiting a characteristic diffraction pattern with the intensity mainly focused in the outer lobes. This phenomenon, called the discrete diffraction of light [2] was theoretically and experimentally observed in one-dimensional (1D) waveguide arrays [3] and two-dimensional (2D) photonic lattices [4]. It is also investigated in aperiodic photonic lattices [5–8] as well as in other systems, such as atomic photonic lattices [9–11].

The truncation of periodic photonic lattice causes an additional distortion in the periodicity and results in the formation of optical surface states that are analogous to the surface states in the electronic theory of periodic systems [12,13]. Optical self-trapped discrete surface waves - surface solitons - have been demonstrated in 1D waveguide arrays [14,15] and in 2D photonic lattices [16]. Physical systems with dimensionality crossover have attracted huge attention, for example, the continuous transformation of photonic lattice from one dimension to two dimensions [17]. In such systems, intermediate states can occur that do not exist in either 1D or 2D geometries. For these structures, there are still open questions: How, when and why does a system cross over from one to two dimensions?

Nondiffracting beams are convenient for the generation of 2D photonic lattices, since they can retain propagation-invariant structure even under weak nonlinearity [18]. There are four major nondiffracting beam families that are exact solutions of the Helmholtz equation in different coordinate systems [19,20]: plane waves in Cartesian, Bessel beams in circular cylindrical [21], Mathieu beams in elliptic cylindrical [22], and parabolic beams in parabolic cylindrical coordinates [23]. We opt for Mathieu beams, since they are used for optical lattice-writing that allows solitons or even elliptically shaped vortex solitons [24]. They are also used for the creation

of different aperiodic photonic lattices by the optical induction technique in photorefractive crystals [8,25], as well as for particle manipulation [26].

In this paper, we investigate the conditions for discrete diffraction occurrence and its properties in the aperiodic Mathieu photonic lattices, both experimentally and theoretically. Owing to their shape, Mathieu beams enable one-pass experimental realization of naturally *truncated aperiodic* photonic lattices, supporting *surface states* as well as discrete diffraction on the surface. We focus on the aperiodic photonic structures in elliptical-radial geometries, since they offer a broad range of shapes, including ellipticity as an additional degree of freedom. They also allow to raise the question on the dimensionality of discrete diffraction. For difference, in periodic photonic lattices there are only two parameters affecting discrete diffraction: the lattice period and the refractive index modulation depth, and they are uniform over the whole lattice. However, the lattice period and the refractive index modulation of Mathieu lattices are not independent parameters; they are connected via Mathieu beam parameters (the beam order, characteristic structural size, and the ellipticity of the beam). Due to the aperiodicity of Mathieu lattice, there are various probing local environments supporting discrete diffraction influenced by the nearest neighbors. During the propagation, diffracting probe can pass through changed local enviroments, unlike in the periodic lattice, causing additional variations in the discrete diffraction effects.

Here, we demonstrate elliptical-radial discrete diffraction in photonic lattices realized by a single Mathieu beam. By changing the order, characteristic structure size, and ellipticity of the Mathieu beam, we are able to control discrete diffraction in the radial direction, as well as the shape of their distributions in the perpendicular directions: circular, elliptic, or hyperbolic. By changing the input probe beam position, we observe switching from the 1D to the 2D discrete diffraction. In our medium - the photorefractive birefringent cerium-doped strontium barium niobate (SBN61:Ce) - the crystal anisotropy plays an important role in the discrete diffraction phenomenon: we observe the most pronounced 2D discrete diffraction along the crystal anisotropy direction.

2. Numerical modeling and experimental realization of light propagation in Mathieu photonic lattices

We investigate the light propagation in Mathieu photonic lattices in the photorefractive medium and study the conditions for the discrete diffraction of light in such lattices. We model linear light propagation in a photonic lattice by solving the coupled system of two equations: the nonlinear Schrödinger equation for the scalar electric field, as the propagation equation, and the diffusion equation for the electrostatic potential as the potential equation [27,28]. We solve both equations numerically, by employing a spectral split-step beam propagation method [29]. The propagation equation of the scalar electric field A with longitudinal wave vector k_z is given by:

$$i\partial_z A + \frac{1}{2k_z}\Delta_\perp A + \frac{k_z}{2n_{o,e}^2}\delta n^2 A = 0, \tag{1}$$

where the wave number $k = 2\pi/\lambda = \sqrt{(k_\perp^2 + k_z^2)}$ is defined by the laser wavelength $\lambda = 532$nm. The potential in the propagation equation is specified by $\delta n^2 = -n_{o,e}^4 r_{13,33}E$, where $n_e = 2.325$ and $n_o = 2.358$ are the extraordinary and ordinary indices, and $r_{13} = 47$pm/V and $r_{33} = 237$pm/V are the corresponding electro-optic coefficients of the birefringent SBN61:Ce crystal. The total electric field $E = E_{ext} + E_{sc}$ that builds up inside the crystal is a superposition of an external electric field $E_{ext} = 2000$V/cm aligned with the optical $c = x$ axis and an internal space charge field E_{sc} that results from the incident intensity distribution within the potential equation.

In order to take the electric bias of the crystal into account and the photorefractive material response, we implement an anisotropic potential equation for the spatial evolution of the

electrostatic potential ϕ_{sc} of the optically-induced space-charge field E_{sc}

$$\Delta_\perp \phi_{sc} + \nabla_\perp \ln(1+I) \cdot \nabla_\perp \phi_{sc} = E_{ext} \partial_x \ln(1+I), \qquad (2)$$

where $I = |A|^2$ is obtained from Eq. 1. Subsequently, Eq. 1 is updated with the optically induced space-charge field

$$E_{sc} = \partial_x \phi_{sc}, \qquad (3)$$

obtained by solving Eq. 2. This procedure is iteratively repeated along the propagation direction.

The process of generation of the propagation-invariant Mathieu photonic lattice is modeled through the distribution $I = I_{latt}$ from Eq. (2), which we refer to as the writing lattice pattern in the experiment [25]. Thus, we obtain first the spatial distribution of I_{latt} in a separate numerical simulation of Eqs. (1) and (2), by propagating an ordinary Mathieu beam in the weak nonlinear case. Then we use such a nearly diffractionless lattice distribution as a lattice potential, to simulate an extraordinary Gaussian probe beam propagation. For this, we use the same equations but with the modified total intensity distribution $I = I_p + I_{latt}$, where the Gaussian probe beam intensity $I_p = |A|^2$ is obtained from Eq. 1. In our simulations with the probe beam, I_p is kept sufficiently weak, so as not to cause an excessive nonlinear modification.

To experimentally investigate the linear light propagation of narrow probe Gaussian beam in Mathieu photonic lattices, we use the experimental setup shown in Fig. 1. As a light source, we use a frequency-doubled Nd:YVO$_4$ laser that emits continuous wave laser light at a wavelength of $\lambda = 532$nm. The expanded and collimated laser beam (telescope L1-L2) illuminates as a plane wave the phase-only spatial light modulator (SLM). Both the amplitude and phase of the reflected light field are modulated. This is accomplished by addressing to the SLM a precalculated hologram containing the information on the complex light field of the Mathieu lattice, encoded with an additional blazed grating [25,30]. In this way, an ordinary polarized beam is spatially modulated and we use it as the writing beam. We demagnify it by a telescope (L3-L4), to illuminate a crystal. The diffraction pattern of the Mathieu lattice is bandpass filtered in Fourier space (FF) [30]. The SBN61:Ce crystal with dimensions of $5 \times 5 \times 20$mm^3 is externally biased with an electric field of E_{ext} aligned with the optical $c = x$ axis, perpendicular to the direction of propagation, z axis, and parallel to the long axis of the crystal. As a result, the ordinary polarized beam optically induces a refractive index modulation, using the lattice writing beam power P, corresponding to the numerically calculated Mathieu lattice. After the fabrication of the Mathieu lattice, the writing beam and the external electric field are switched off. Then an extraordinary polarized narrow Gaussian probe beam illuminates the specified lattice position and we observe linear light propagation in the Mathieu photonic lattice. A half-wave plate rotates the probe beam's linear polarization by 90° relative to the writing beam's polarization, addressing the
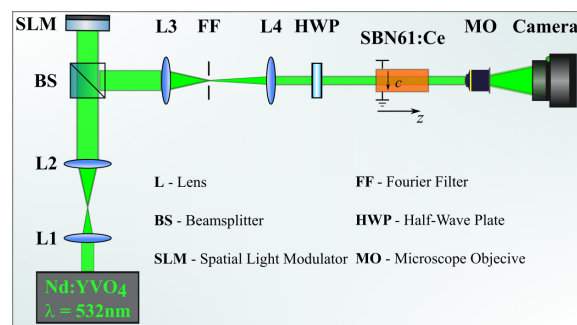
Fig. 1. Experimental setup for the light beam propagation investigation in the two-dimensional Mathieu photonic lattice.

stronger electro-optic coefficient. We use an imaging system formed by a microscope objective (MO) with the camera to detect the transverse intensity distribution of the writing and/or probing beam at the back face of the crystal. A low probe beam's power keeps the propagation in a linear regime, and the lattice refractive index modulation remains unmodified (until erased by white light). The probe beam of full-width-at-half-maximum of 8μm is directly positioned in front of the crystal and its transverse position defines the input center. We determine the beam size to be adequate to illuminate one lattice site.

3. Transition from 1D to 2D discrete diffraction

Mathieu beams are a class of nondiffracting beams suitable for the realization of photonic lattices. We base our study on even Mathieu beams $M_m(\xi, \eta)$ of order m, which are mathematically described as a product of the radial c_{em} and angular J_{em} Mathieu functions of order m: $M_m(\xi, \eta) = C_m(q)J_{em}(\xi; q)c_{em}(\eta; q)$. Here, $C_m(q)$ is a weighting constant that depends on the ellipticity parameter $q = f^2 k_t^2/4$ that is related to the positions of the two foci f and the transverse wave number $k_t = 2\pi/a$, where a is the characteristic structure size. Elliptical coordinates (ξ, η) are related to the Cartesian coordinates (x, y) by $x + iy = f cosh(\xi + i\eta)$. Mathieu beams M_m are used for generating lattice intensity distribution I_{latt} by numerical simulation of Eq. 1 and Eq. 2. By changing some of the main characteristics of Mathieu beams, defined by the parameters: beam order m, ellipticity q, and characteristic structure size a, we are capable of managing various spatial intensity distributions of Mathieu lattices [25]. The refractive index change and the lattice period of such a lattice are not independent parameters, but are connected via Mathieu beam parameters m, q, and a. Various probing local environments in Mathieu lattices support the formation of different discrete diffraction patterns. By changing the ellipticity of the Mathieu lattice, one changes the curvature of the lines connecting nearest neighbour sites (which is zero in the periodic lattice), thus influencing discrete diffraction patterns. Similarly, the anisotropy of our medium (SBN61:Ce crystal) enables the conditions for supporting discrete diffraction in certain directions.

We start by using Mathieu lattice with zero ellipticity ($q = 0$), where the waveguide arrays are distributed along the circles, as well as along the radial spikes. Three input probe beam positions are chosen, shown in Fig. 2(a1), (1, 2, and 3) marked with yellow arrows for the sites at the first, second, and fourth circle waveguide arrays, respectively. All 3 positions belong to the same radial spike, while positions 4 and 5 (the green arrows) belong to the most intense first circular waveguide. We compare the numerical and experimental results of the probe beam intensity distributions at the crystal back face after 2 *cm* propagation. For the first input probe beam position on the lattice edge (marked as position 1 in Fig. 2(a1)), we observe behavior similar to the 2D discrete diffraction. We will refer to it as the radial 2D discrete diffraction in the truncated elliptical-radial lattice (Fig. 2(b1),(b2)). On the same circular waveguide array, but on the opposite side of the input probe beam position, we notice out-of-order appearance of intensive spots collecting evanescent leakage of the waveguides from the opposite side.

Following the geometrical distribution of the lattice, we show the projection of the probe beam intensity distributions on the circle and spike waveguide arrays (the corresponding circles and spikes are marked in Fig. 3(a)) along the propagation distance. In the circular direction, we cut the first four circles opposite to the excitation position and show flattened probe intensity distributions in Fig. 3(b), presenting discrete diffraction along circles. On the edges of Fig. 3(b) distribution, corresponding to the cut point, we can follow the dynamics of the previously mentioned opposite intensive spot. In the radial direction, we notice discrete edge diffraction along some of the truncated spike waveguide arrays (Fig. 3(c)). When we shift the probe beam input position away from the lattice edge (position 2 in Fig. 2(a1)), the two-dimensionality of discrete diffraction is less pronounced, but at the expense of separate circular and radial 1D discrete diffractions. For the third probe beam position (position 3 in Fig. 2(a1)), we notice separate circular and radial
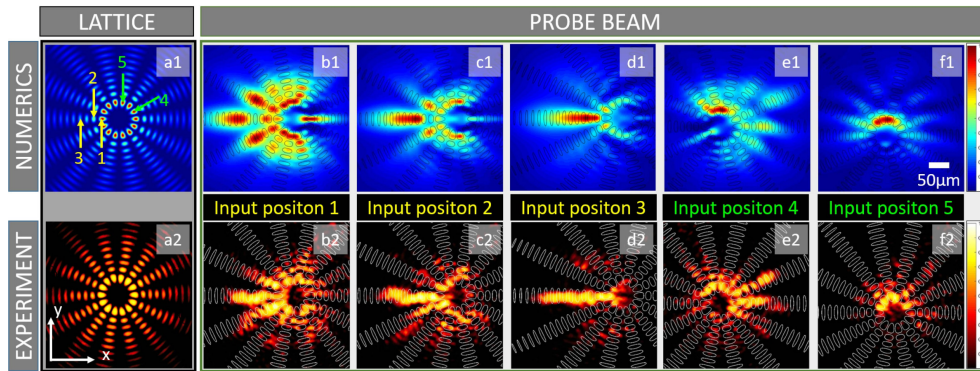
Fig. 2. Influence of various probe beam input positions on the discrete diffraction in Mathieu lattice. The intensity distribution of the Mathieu lattice at the exit crystal face observed numerically (a1) and experimentally (a2), with yellow arrows in (a1) indicating various input probe beam positions. Intensity distributions of the probe beam at the exit crystal face obtained numerically (the first row) for the input probe beam positions: 1 (b1), 2 (c1), 3 (d1), 4 (e1), and 5 (f1), taken from Visualization 1, Visualization 2, Visualization 3, Visualization 4 and Visualization 5, respectively, representing the numerical intensity distributions of the probe beam along the propagation direction. Experimentally obtained intensity distributions at the crystal exit face (the second row) for input probe beam positions: 1 (b2), 2 (c2), 3 (d2), 4 (e2), and 5 (f2). Parameters are: Mathieu lattice order m = 7, ellipticity $q = 0$, and characteristic structure size $a = 30\mu m$, $I_{latt} = 1$, experimental lattice writing beam power $P = 0.5mW$.

discrete diffractions. Hence, we observe the switching from 2D to 1D discrete diffraction in truncated elliptical-radial lattice, by changing the input probe beam position.

Additionally, we investigate the influence of crystal anisotropy on light diffraction in such a lattice (Fig. 2). We consider various input probe beam positions, depicted as positions 1, 4, and 5 in Fig. 2(a1): All input beam positions are on the same circular waveguide array and would be equivalent, apart from the relative orientation to the crystal anisotropy. As one can see, in such lattices 2D discrete diffraction is possible to observe *only* for input probe beam positions along the crystal anisotropy direction (*c*-axis) (Fig. 2(b)).

With increasing Mathieu lattice order *m*, the number of spike waveguide arrays is increased, favoring 2D discrete diffraction (Fig. 4(a-c)). We study the probe beam propagation for three
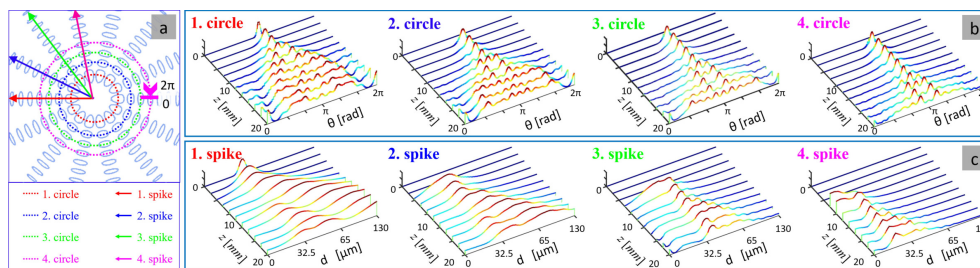

Fig. 3. Discrete diffraction along the circular and spike waveguide arrays. Projections of intensity distributions along circles (b), and spikes (c) corresponding to (a). For each circle, the circumference is measured in the angular coordinate θ starting from the cut point, and the radial coordinate d from the common center of the circles. The parameters are as in Fig. 2(b1).

lattice orders: $m = 7, 9$, and 12, and obtain more pronounced 2D discrete diffraction for higher lattice order. Also, we study how the variation of the Mathieu lattice characteristic structure size a influences the propagation of the probe beam: Increasing the characteristic structure size a uniformly increases the distance between neighboring sites (Fig. 4(c-e)). We are able to control optimal conditions for 2D or more 1D discrete diffractions in certain regions, and with the variation of structure size a, we are able to move those regions. We investigate Mathieu lattices for three characteristic structure sizes: $a = 30, 35$, and $40 \mu m$. 2D discrete diffraction becomes less pronounced with the increase of a, which is caused by the increasing order separation in each concentric elliptical waveguide array.
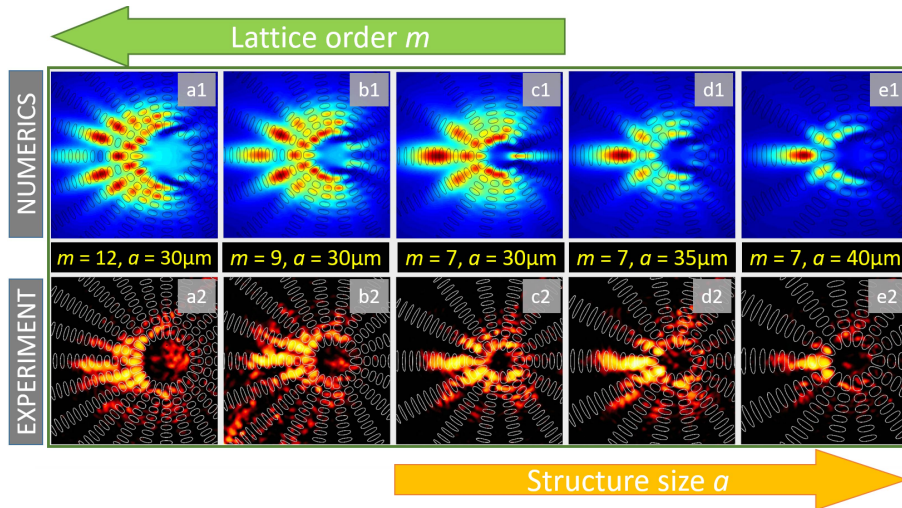
Fig. 4. Influence of Mathieu lattices order m and structural size a on the discrete diffraction patterns. (a1-e1) Numerically observed intensity distributions of the probe beam at the exit crystal face for different parameters m, a, marked in each panel, and $q = 5$, taken from Visualization 6, Visualization 7, Visualization 8, Visualization 9, Visualization 10, respectively. The second row presents the corresponding experimental exit face intensity distributions (a2-e2). Other parameters are as in Fig. 2.

At the end, we study how the variation of Mathieu lattice ellipticity q influences the discrete diffraction of light (Fig. 5). We perform our investigation by probing Mathieu lattices with various ellipticities: $q = 0, 10, 125$, and 625. Probe beam input positions are marked with the yellow arrows depicted in Fig. 5 (the first row). For ellipticity $q = 0$, we notice 2D radial discrete diffraction, in contrast to the ellipticity of $q = 10$, where one notices the splitting to 1D radial discrete diffractions along the inner ellipse and the left spike waveguide array. With further increasing q, due to modulation depth distributions - i.e., nonuniform distributions, favorable conditions for discrete diffraction appear for high q, where we have hyperbolic lattices. For ellipticity $q = 125$, we obtain 2D discrete diffraction across hyperbolas, while for $q = 625$, we observe more 1D discrete diffraction along the edge hyperbola, mostly due to the sharp decrease of array intensity distribution away from the edge hyperbola. As stated, the distribution is rapidly decaying away from the edge row, which in the absence of anisotropy would result in dominantly 1D discrete diffraction (not shown).
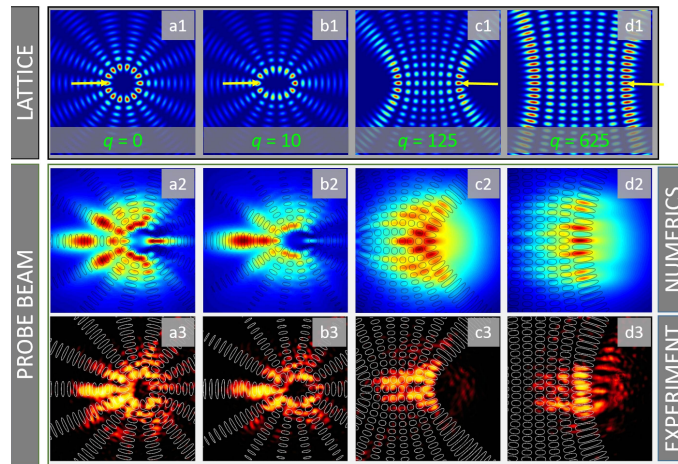
Fig. 5. Lattice ellipticity q influence on the discrete diffraction of light. First row: Intensity distributions of Mathieu lattice. Second row: probe beam intensity distributions at the exit face of the crystal, obtained numerically (a2- d2), taken from the corresponding numerical intensity distributions of the probe beam along the propagation direction: Visualization 1, Visualization 11, Visualization 12, Visualization 13, respectively. The third row: Experimental intensity distributions of the probe beam at the crystal exit face (a3-d3). Other parameters are as in Fig. 2.

4. Conclusion

In summary, we have presented a method for radial and angular discrete diffraction generation in various Mathieu lattices, experimentally and numerically. Such photonic lattices are optically induced in a photorefractive crystal, using one-pass creation in the experiment. They are also a kind of truncated lattices that could support surface states. Mathieu photonic structures offer an extensive variation of shapes as well as ellipticity, as the additional degree of freedom, with the waveguides deployed along circles, ellipses, and hyperbolas, as well as radial spikes. We have controlled radial discrete diffraction by changing the order, characteristic structure size, and ellipticity of Mathieu beams used for the optical induction of photonic lattices. Shifting the input probe beam position, we have observed a transition from 1D to 2D discrete diffraction. We have found the most pronounced 2D discrete diffraction along the crystal anisotropy direction. Note that the discrete diffraction created by our approach exhibits branching 1D discrete diffraction along circle/ellipse and spike waveguide arrays, while predominantly 1D discrete diffraction occurs in hyperbolic lattices. Our results pave the way for exploiting light propagation in a novel class of optical lattices, but they are not limited to these particular lattices: They can readily be generalized in other kinds of optically induced lattices. Adaptivity and reconfigurability of the light-guiding structures play an important role in enabling functionality, displaying a significant advance in modern photonics and providing an important step towards novel innovative wave-guiding applications and light routing approaches. They will hopefully find useful applications in the capacity-enhanced optical information processing.

Data availability. Data underlying the results presented in this paper are not publicly available at this time but may be obtained from the authors upon reasonable request.

References

1. F. Lederer, G. I. Stegeman, D. N. Christodoulides, G. Assanto, and M. S. Y. Silberberg, "Discrete solitons in optics," Phys. Rep. **463**(1-3), 1–126 (2008).
2. D. N. Christodoulides, F. Lederer, and Y. Silberberg, "Discretizing light behaviour in linear and nonlinear waveguide lattices," Nature **424**(6950), 817–823 (2003).
3. T. Pertsch, T. Zentgraf, U. Peschel, A. Bräuer, and F. Lederer, "Anomalous refraction and diffraction in discrete optical systems," Phys. Rev. Lett. **88**(9), 093901 (2002).
4. J. W. Fleischer, M. Segev, N. K. Efremidis, and D. N. Christodoulides, "Observation of two-dimensional discrete solitons in optically induced nonlinear photonic lattices," Nature **422**(6928), 147–150 (2003).
5. Z. Vardeny, A. Nahata, and A. Agrawal, "Optics of photonic quasicrystals," Nat. Photonics **7**(3), 177–187 (2013).
6. L. Negro and S. Boriskina, "Deterministic aperiodic nanostructures for photonics and plasmonics applications," Laser Photonics Rev. **6**(2), 178–218 (2012).
7. M. Boguslawski, N. M. Lučić, F. Diebel, D. V. Timotijević, C. Denz, and D. M. J. Savić, "Light localization in optically induced deterministic aperiodic fibonacci lattices," Optica **3**(7), 711–717 (2016).
8. J. M. Vasiljević, A. Zannotti, D. V. Timotijević, C. Denz, and D. M. J. Savić, "Light propagation in aperiodic photonic lattices created by synthesized mathieu–gauss beams," Appl. Phys. Lett. **117**(4), 041102 (2020).
9. J. Yuan, H. Zhang, C. Wu, G. Chen, L. X. Lirong Wang, and S. Jia, "Creation and control of vortex-beam arrays in atomic vapor," Laser Photonics Rev. **17**, 2200667 (2023).
10. H. Zhang, J. Yuan, L. Xiao, S. Jia, and L. Wang, "Geometric pattern evolution of photonic graphene in coherent atomic medium," Opt. Express **31**(7), 11335–11343 (2023).
11. J. Yuan, C. Wu, L. Wang, G. Chen, and S. Jia, "Observation of diffraction pattern in two-dimensional optically induced atomic lattice," Opt. Lett. **44**(17), 4123–4126 (2019).
12. Y. S. Kivshar, "Nonlinear tamm states and surface effects in periodic photonic structures," Laser Phys. Lett. **10**, 703–713 (2008).
13. S. Suntsov, K. G. Makris, G. A. Siviloglou, R. Iwanow, R. Schiek, D. N. Christodoulides, G. I. Stegeman, R. Morandotti, H. Yang, G. Salamo, M. Volatier, V. Aimez, R. Arès, M. Sorel, Y. Min, W. Sohler, X. Wang, A. Bezryadina, and Z. Chen, "Observation of one- and two-dimensional discrete surface spatial solitons," J. Nonlinear Optic. Phys. Mat. **16**(04), 401–426 (2007).
14. K. G. Makris, S. Suntsov, D. N. Christodoulides, G. I. Stegeman, and A. Hache, "Discrete surface solitons," Opt. Lett. **30**(18), 2466–2468 (2005).
15. C. R. Rosberg, D. N. Neshev, W. Krolikowski, A. Mitchell, R. A. Vicencio, M. I. Molina, and Y. S. Kivshar, "Observation of surface gap solitons in semi-infinite waveguide arrays," Phys. Rev. Lett. **97**(8), 083901 (2006).
16. X. Wang, A. Bezryadina, Z. Chenand, K. G. Makris, D. N. Christodoulides, and G. I. Stegeman, "Observation of two-dimensional surface solitons," Phys. Rev. Lett. **98**(12), 123903 (2007).
17. A. Szameit, Y. V. Kartashov, F. Dreisow, M. Heinrich, T. Pertsch, S. Nolte, A. Tünnermann, V. A. Vysloukh, F. Lederer, and L. Torner, "Soliton excitation in waveguide arrays with an effective intermediate dimensionality," Phys. Rev. Lett. **102**(6), 063902 (2009).
18. A. Zannotti, J. M. Vasiljević, D. V. Timotijević, D. M. J. Savić, and C. Denz, "Morphing discrete diffraction in nonlinear mathieu lattices," Opt. Lett. **44**(7), 1592–1595 (2019).
19. M. V. Berry and N. L. Balazs, "Nonspreading wave packets," Am. J. Phys. **47**(3), 264–267 (1979).
20. E. G. Kalnins and J. W. Miller, "Lie theory and separation of variables. 9. orthogonal r-separable coordinate systems for the wave equation $\psi_{tt} - \triangle_2 \psi = 0$," J. Math. Phys. **17**(3), 331–355 (1976).
21. J. Durnin, J. J. Miceli, and J. H. Eberly, "Diffraction-free beams," Phys. Rev. Lett. **58**(15), 1499–1501 (1987).
22. J. C. Gutiérrez-Vega, M. D. Iturbe-Castillo, and S. Chávez-Cerda, "Alternative formulation for invariant optical fields: Mathieu beams," Opt. Lett. **25**(20), 1493–1495 (2000).
23. M. A. Bandres, J. C. Gutiérrez-Vega, and S. Chávez-Cerda, "Parabolic nondiffracting optical wave fields," Opt. Lett. **29**(1), 44–46 (2004).
24. J. M. Vasiljević, A. Zannotti, D. V. Timotijević, C. Denz, and D. M. Jović Savić, "Elliptical vortex necklaces in mathieu lattices," Phys. Rev. A **97**(3), 033848 (2018).
25. J. V. Vasiljević, A. Zannotti, D. V. Timotijević, C. Denz, and D. M. J. Savić, "Creating aperiodic photonic structures by synthesized mathieu-gauss beams," Phys. Rev. A **96**(2), 023840 (2017).
26. K. Dholakia and T. Čižmár, "Shaping the future of manipulation," Nat. Photonics **5**(6), 335–342 (2011).
27. A. A. Zozulya and D. Z. Anderson, "Propagation of an optical beam in a photorefractive medium in the presence of a photogalvanic nonlinearity or an externally applied electric field," Phys. Rev. A **51**(2), 1520–1531 (1995).
28. D. V. Timotijević, J. M. Vasiljević, and D. M. J. Savić, "Numerical methods for generation and characterization of disordered aperiodic photonic lattices," Opt. Express **30**(5), 7210–7224 (2022).
29. G. Agrawal, *Nonlinear Fiber Optics*, 5th ed (Academic Press, 2012).
30. J. A. Davis, D. M. Cottrell, J. Campos, M. J. Yzuel, and I. Moreno, "Encoding amplitude information onto phase-only filters," Appl. Opt. **38**(23), 5004–5013 (1999).